Electronic Supplementary Material (ESI) for Dalton Transactions

Supplementary Information

ε-Keggin -based coordination networks: synthesis, structure and application toward green synthesis of polyoxometalate@graphene hybrids

L. Marleny Rodriguez Albelo,[a] Guillaume Rousseau,[b] Pierre Mialane,[b] Jérôme Marrot,[b] Caroline Mellot-Draznieks,[c] A. Rabdel Ruiz-Salvador,[a] Shiwen Li,[d] Rongji Liu,[e] Guangjin Zhang,[e] Bineta Keita,*[,d] and Anne Dolbecq*[,b]

Experimental section for the POM@G hybrids synthesis and characterizations

Reagents, Apparatus and procedures

The composition of the aqueous electrolyte was 1M LiCl + HCl (pH 1). The electrochemical set-up was an EG & G 273 A potentiostat driven by a PC with the M270 software. For electrochemical experiments, the source, mounting and polishing of the glassy carbon (3 mm diameter) electrodes (Le Carbone Lorraine, France) have been described previously.[1] Potentials are measured against a saturated calomel reference electrode (SCE). The counter electrode was a platinum gauze of large surface area. Pure water from a RiOs 8 unit followed by a Millipore-Q Academic purification set was used throughout. The solutions were deaerated thoroughly for at least 30 minutes with pure argon and kept under a positive pressure of this gas during the experiments. Controlled potential coulometry experiments were carried out with a large surface area carbon plate.

Synthesis of graphite oxide (GO)

GO was prepared from nature G flakes by a modified Hummers method as described everywhere.[2] As synthesized GO (6.25ml ,0.8mg mL^{-1}) was diluted in 250 ml water and sonicated 30 min to form a 0.1mg ml^{-1} exfoliated GO dispersion. Ultrapure water purified with Milli-Q (MQ) plus system (Millipore Co.) with resistivity of 18.2 MΩcm was used in all experiments. The brown GO dispersion was further purificated by centrifugation at 3000 rpm for 30 min to remove any unexfoliated GO.[3] The exfoliated GO dispersion is very stable in water.

Preparation of Polyoxometalate@Graphene hybrids (POM@G)

The POM @G hybrids was prepared by adding 125.3 mg **ε(isop)$_2$** to 41.5 ml GO followed by stirring for at least 6 h at room temperature. The samples were then centrifuged at 16000 rpm for 10 min and washed with water 4 times. The samples were then dried in the oven at 80°C.

Preparation of the modified electrodes

The **POM@G-Nafion** electrodes were prepared as previously described.[4] Typically, an electrode is fabricated by depositing 3 μL of the **POM@G** suspension in water (9.5 mg mL^{-1})

on the polished glassy carbon electrode surface, letting it dry in air, then covering with 2 μL of 5 wt% Nafion solution and letting it dry again in air. An alternative procedure consisting of adding the Nafion solution to the **POM@G** suspension in water prior to its deposition on the electrode surface could also be used.

Experimental conditions for TEM, SEM, XPS and Raman Characterizations of POM@G nanohybrids

TEM images were obtained using a JEM-2010 transmission electron microscope at an acceleration voltage of 200 kV. SEM analysis was performed on a Hitachi model JSM 6700F field-emission scanning electron microscope (FESEM). XPS measurements were performed in ultrahigh vacuum (UHV) with Krato, AXIS-HS monochromatized Al K α cathode source, at 75–150 W, using a low-energy electron gun for charge neutralization. Raman spectra were obtained with a Renishaw Raman system model 1000 ectrometer. The 532 nm radiation from a 20 mW air-cooled argon ion laser was used as the exciting source. The laser diameter was 1 μ m, and the laser power at the sample position was 4.0 mW. The data acquisition time was 10 s.

References

[1] B. Keita and L. Nadjo, *J. Electroanal. Chem.*, 1988, **243**, 87.

[2] W. S. Hummers and R. E. Offeman, *J. Am. Chem. Soc.* 1958, **80**, 1339

[3] D. Li, M.B. Muller, S. Gilje, R.B. Kaner and G.G. Wallace, *Nature Nanotechnology*, 2008, **3**, 101.

[4] B. Nohra, H. El Moll, L. M. Rodriguez Albelo, P. Mialane, J. Marrot, C. Mellot-Draznieks, M. O'Keeffe, R. Ngo Biboum, J. Lemaire, B. Keita, L. Nadjo, and A. Dolbecq, *J. Am. Chem. Soc.*, 2011, **133**, 13363.

Figure SI1. Ball and stick representation with partial atomic labeling scheme, selected bond distances (Å) and bond valence summations (BVS) of **ε(isop)$_2$**.

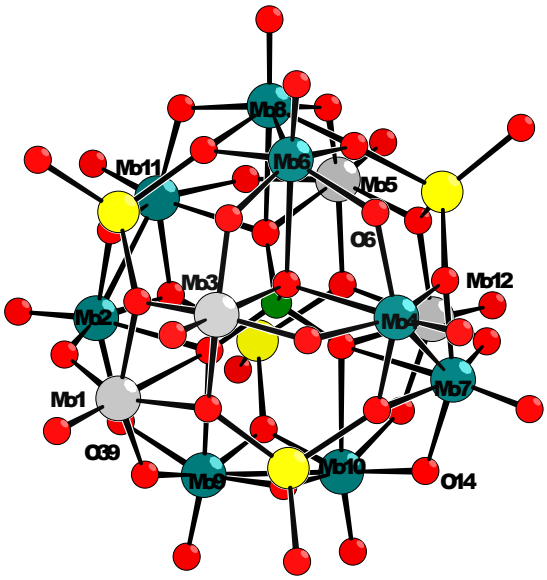

	Distances	BVS
Mo(1)-O(33)	1.683(7)	**Σ(Mo1) = 6.0**
Mo(1)-O(20)	1.818(7)	
Mo(1)-O(25)	1.847(6)	
Mo(1)-O(21)	2.004(6)	
Mo(1)-O(4)	2.007(7)	
Mo(1)-O(19)	2.586(7)	
Mo(1)-Mo(3)	**3.1981(12)**	**=> Mo^{VI}**
Mo(2)-O(45)	1.656(7)	**Σ(Mo2) = 5.3**
Mo(2)-O(13)	1.936(7)	
Mo(2)-O(31)	1.984(8)	
Mo(2)-O(25)	1.998(7)	
Mo(2)-O(39)	2.047(8)	
Mo(2)-O(19)	2.605(7)	
Mo(2)-Mo(11)	**2.6208(12)**	**=> Mo^{V}**
Mo(3)-O(5)	1.679(7)	**Σ(Mo3) = 6.0**
Mo(3)-O(15)	1.815(6)	
Mo(3)-O(40)	1.828(7)	
Mo(3)-O(4)	2.006(6)	
Mo(3)-O(21)	2.036(8)	
Mo(3)-O(24)	2.559(7)	=> **Mo^{VI}**
Mo(4)-O(37)	1.681(7)	**Σ(Mo4) = 5.2**
Mo(4)-O(1)	1.959(6)	
Mo(4)-O(12)	1.955(7)	
Mo(4)-O(15)	2.013(7)	
Mo(4)-O(6)	2.052(7)	
Mo(4)-O(24)	2.602(7)	
Mo(4)-Mo(7)	**2.6089(12)**	**=> Mo^{V}**
Mo(5)-O(11)	1.694(8)	**Σ(Mo5) = 5.9**
Mo(5)-O(22)	1.823(7)	
Mo(5)-O(23)	1.824(7)	
Mo(5)-O(9)	2.034(7)	
Mo(5)-O(18)	2.048(7)	
Mo(5)-O(2)	2.562(7)	
Mo(5)-Mo(12)	**3.1936(13)**	**=> Mo^{VI}**
Mo(6)-O(34)	1.657(8)	**Σ(Mo6) = 5.3**
Mo(6)-O(17)	1.948(7)	
Mo(6)-O(3)	1.973(6)	
Mo(6)-O(40)	1.985(7)	
Mo(6)-O(6)	2.066(6)	
Mo(6)-O(24)	2.547(7)	
Mo(6)-Mo(8)	**2.6052(12)**	**=> Mo^{V}**
Mo(7)-O(36)	1.681(8)	**Σ(Mo7) = 5.2**
Mo(7)-O(1)	1.934(7)	
Mo(7)-O(26)	1.989(8)	
Mo(7)-O(12)	1.989(7)	
Mo(7)-O(14)	2.064(7)	
Mo(7)-O(10)	2.586(8)	=> **Mo^{V}**
Mo(8)-O(43)	1.655(8)	**Σ(Mo8) = 5.3**
Mo(8)-O(17)	1.955(7)	
Mo(8)-O(3)	1.962(7)	
Mo(8)-O(22)	1.979(8)	
Mo(8)-O(8)	2.077(7)	
Mo(8)-O(2)	2.569(7)	=> **Mo^{V}**
Mo(9)-O(42)	1.672(9)	**Σ(Mo9) = 5.3**
Mo(9)-O(16)	1.944(7)	
Mo(9)-O(7)	1.961(7)	
Mo(9)-O(20)	1.994(8)	
Mo(9)-O(39)	2.068(7)	
Mo(9)-O(19)	2.529(7)	
Mo(9)-Mo(10)	**2.6112(13)**	**=> Mo^{V}**
Mo(10)-O(41)	1.652(9)	**Σ(Mo10) = 5.4**
Mo(10)-O(7)	1.930(7)	
Mo(10)-O(16)	1.952(7)	
Mo(10)-O(28)	1.989(8)	
Mo(10)-O(14)	2.081(7)	
Mo(10)-O(10)	2.578(7)	=> **Mo^{V}**
Mo(11)-O(32)	1.691(7)	**Σ(Mo11) = 5.1**
Mo(11)-O(31)	1.949(8)	
Mo(11)-O(13)	1.965(7)	
Mo(11)-O(23)	2.016(7)	
Mo(11)-O(8)	2.079(7)	
Mo(11)-O(2)	2.580(7)	=> **Mo^{V}**
Mo(12)-O(29)	1.693(8)	**Σ(Mo12) = 5.9**
Mo(12)-O(26)	1.838(8)	
Mo(12)-O(28)	1.850(8)	
Mo(12)-O(9)	1.989(7)	
Mo(12)-O(18)	2.019(6)	
Mo(12)-O(10)	2.560(7)	=> **Mo^{VI}**

Σ(O6) = 1.3 => OH, **Σ(O14) = 1.3** => OH, **Σ(O39) = 1.3** => OH

Figure SI2. Ball and stick representation with partial atomic labeling scheme, selected bond distances (Å) and bond valence summations (BVS) of **TPA[ε(trim)]**$_\infty$.

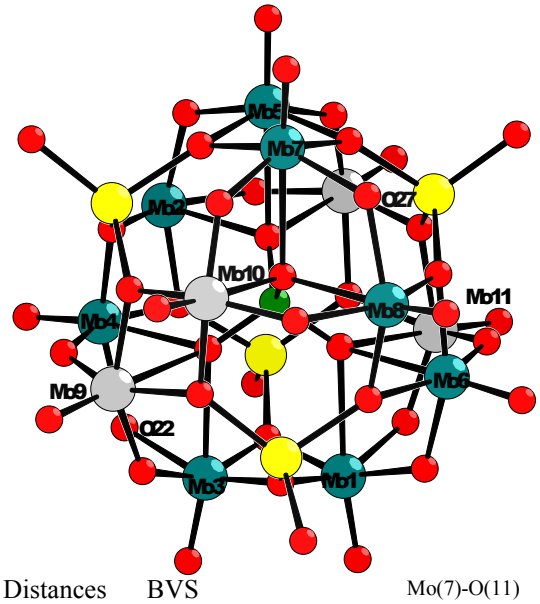

	Distances	BVS
Mo(1)-O(32)	1.679(4)	**Σ(Mo1) = 5.3**
Mo(1)-O(17)	1.959(4)	
Mo(1)-O(16)	1.969(4)	
Mo(1)-O(26)	1.986(4)	
Mo(1)-O(1)	2.008(4)	
Mo(1)-O(7)	2.550(4)	
Mo(1)-Mo(3)	**2.6157(8)**	**=> Mo^{V}**
Mo(2)-O(41)	1.677(4)	**Σ(Mo2) = 5.2**
Mo(2)-O(3)	1.938(4)	
Mo(2)-O(14)	1.977(4)	
Mo(2)-O(15)#1	2.010(4)	
Mo(2)-O(33)	2.047(4)	
Mo(2)-O(28)	2.539(4)	
Mo(2)-Mo(4)	**2.6209(8)**	**= > Mo^{V}**
Mo(3)-O(20)	1.664(4)	**Σ(Mo3) = 5.3**
Mo(3)-O(17)	1.937(4)	
Mo(3)-O(16)	1.960(4)	
Mo(3)-O(31)	1.999(4)	
Mo(3)-O(22)	2.087(4)	
Mo(3)-O(5)	2.543(4)	**=> Mo^{V}**
Mo(4)-O(18)	1.669(4)	**Σ(Mo4) = 5.2**
Mo(4)-O(3)	1.959(4)	
Mo(4)-O(14)	1.958(4)	
Mo(4)-O(37)	2.012(4)	
Mo(4)-O(22)	2.068(4)	
Mo(4)-O(5)	2.569(4)	**=> Mo^{V}**
Mo(5)-O(43)	1.678(4)	**Σ(Mo5) = 5.3**
Mo(5)-O(19)	1.947(4)	
Mo(5)-O(6)	1.950(4)	
Mo(5)-O(34)	2.010(4)	
Mo(5)-O(15)#1	2.010(4)	
Mo(5)-O(28)	2.5607(4)	
Mo(5)-Mo(7)	2.6170(7)	**=> Mo^{V}**
Mo(6)-O(38)	1.647(4)	**Σ(Mo6) = 5.3**
Mo(6)-O(12)	1.968(4)	
Mo(6)-O(25)	1.974(4)	
Mo(6)-O(1)	2.009(4)	
Mo(6)-O(35)	2.059(4)	
Mo(6)-O(7)	2.544(4)	
Mo(6)-Mo(8)	2.6251(7)	**=> Mo^{V}**
Mo(7)-O(11)	1.661(4)	**Σ(Mo7) = 5.3**
Mo(7)-O(6)	1.949(4)	
Mo(7)-O(19)	1.951(4)	
Mo(7)-O(39)	1.990(4)	
Mo(7)-O(27)	2.073(4)	
Mo(7)-O(7)	2.567(4)	**=> Mo^{V}**
Mo(8)-O(21)	1.667(4)	**Σ(Mo8) = 5.2**
Mo(8)-O(25)	1.936(4)	
Mo(8)-O(12)	1.976(4)	
Mo(8)-O(36)	2.024(4)	
Mo(8)-O(27)	2.095(4)	
Mo(8)-O(9)	2.559(4)	**=> Mo^{V}**
Mo(9)-O(29)	1.699(4)	**Σ(Mo9) = 6.0**
Mo(9)-O(37)	1.804(4)	
Mo(9)-O(31)	1.839(4)	
Mo(9)-O(23)	1.991(4)	
Mo(9)-O(13)	2.007(4)	
Mo(9)-O(5)	2.554(4)	
Mo(9)-Mo(10)	**3.1805(7)**	**=> Mo^{VI}**
Mo(10)-O(30)	1.689(4)	**Σ(Mo10) = 6.1**
Mo(10)-O(36)	1.802(4)	
Mo(10)-O(39)	1.810(4)	
Mo(10)-O(13)	2.001(4)	
Mo(10)-O(23)	2.018(4)	
Mo(10)-O(9)	2.582(4)	**=> Mo^{VI}**
Mo(11)-O(40)	1.705(4)	**Σ(Mo11) = 5.9**
Mo(11)-O(35)	1.810(4)	
Mo(11)-O(26)	1.823(4)	
Mo(11)-O(10)	2.009(4)	
Mo(11)-O(2)	2.026(4)	
Mo(11)-O(7)	2.604(4)	
Mo(11)-Mo(12)	**3.1992(7)**	**=> Mo^{VI}**
Mo(12)-O(24)	1.693(4)	**Σ(Mo12) = 6.1**
Mo(12)-O(33)	1.797(4)	
Mo(12)-O(34)	1.816(4)	
Mo(12)-O(2)	1.993(4)	
Mo(12)-O(10)	1.997(4)	
Mo(12)-O(28)	2.559(4)	**=> Mo^{VI}**

Σ(O22) = 1.2 => OH
Σ(O27) = 1.2 => OH

Figure SI3. Ball and stick representation with partial atomic labeling scheme, selected bond distances (Å) and bond valence summations (BVS) of **ε(bim)$_4$**.

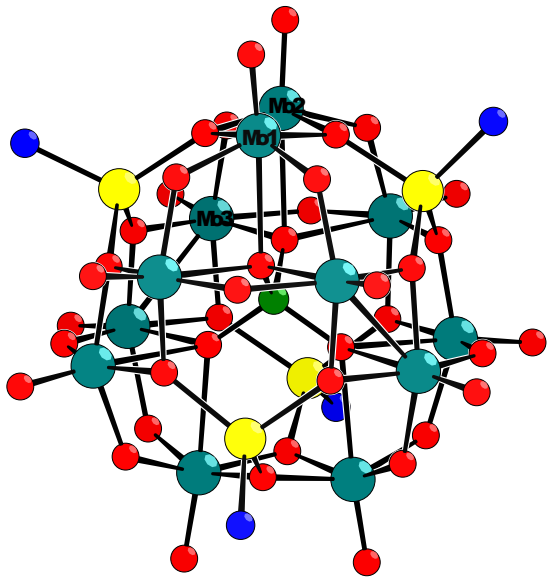

	Distances	BVS
Mo(1)-O(7)	1.626(10)	**Σ(Mo1) = 6.0**
Mo(1)-O(5)	1.893(7)	
Mo(1)-O(9)#1	1.905(7)	
Mo(1)-O(2)	1.955(7)	
Mo(1)-O(3)#1	1.999(7)	
Mo(1)-O(1)	2.551(7)	
Mo(1)-Mo(2)	**2.9869(15)**	
Mo(2)-O(10)	1.679(8)	**Σ(Mo2) = 6.0 => disordered Mo^{V} and Mo^{VI} ions**
Mo(2)-O(6)	1.841(7)	
Mo(2)-O(9)	1.922(7)	
Mo(2)-O(3)#1	1.925(7)	
Mo(2)-O(2)	1.987(7)	
Mo(2)-O(1)	2.498(7)	
Mo(3)-O(8)	1.654(9)	**Σ(Mo3) = 5.7**
Mo(3)-O(4)	1.888(8)	
Mo(3)-O(4)#2	1.964(10)	
Mo(3)-O(5)	1.968(8)	
Mo(3)-O(6)#1	1.978(8)	
Mo(3)-O(3)#1	2.548(7)	
Mo(3)-Mo(3)#2	**2.693(2)**	

Figure SI4. Ball and stick representation with partial atomic labeling scheme, selected bond distances (Å) and bond valence summations (BVS) of **ε(pazo)$_4$**.

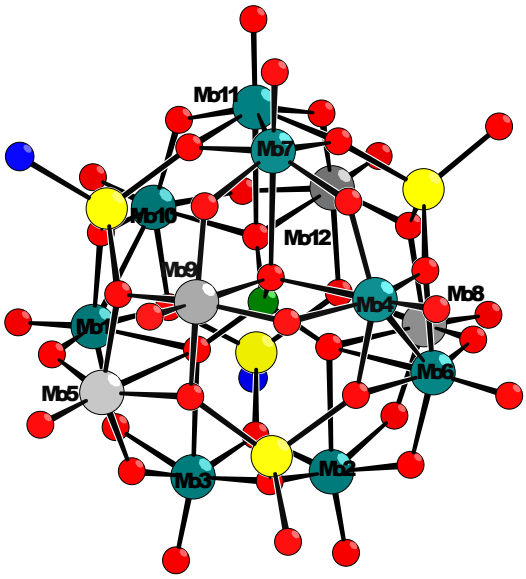

Mo(1)-O(18)	1.690(7)	**Σ(Mo1) = 5.3**
Mo(1)-O(9)	1.934(7)	
Mo(1)-O(26)	1.961(7)	
Mo(1)-O(16)	1.978(7)	
Mo(1)-O(6)	2.028(7)	
Mo(1)-O(23)	2.480(6)	
Mo(1)-Mo(10)	**2.6351(17) => Mo^{V}**	
Mo(2)-O(35)	1.662(7)	**Σ(Mo2) = 5.4**
Mo(2)-O(3)	1.924(6)	
Mo(2)-O(11)	1.971(6)	
Mo(2)-O(1)#1	2.005(6)	
Mo(2)-O(13)	2.037(7)	
Mo(2)-O(4)	2.488(6)	
Mo(2)-Mo(3)	**2.6262(14) => Mo^{V}**	
Mo(3)-O(14)	1.685(7)	**Σ(Mo3) = 5.4**
Mo(3)-O(26)	1.955(7)	
Mo(3)-O(3)	1.960(6)	
Mo(3)-O(11)	1.971(7)	
Mo(3)-O(15)	2.019(7)	
Mo(3)-O(23)	2.536(7) => **Mo^{V}**	
Mo(4)-O(30)	1.665(7)	**Σ(Mo4) = 5.5**
Mo(4)-O(27)	1.937(7)	
Mo(4)-O(10)	1.946(7)	
Mo(4)-O(7)	1.971(7)	
Mo(4)-O(33)	2.003(7)	
Mo(4)-O(5)	2.540(7)	
Mo(4)-Mo(6)	**2.6213(18) => Mo^{V}**	
Mo(5)-O(36)	1.690(7)	**Σ(Mo5) = 6.1**
Mo(5)-O(15)	1.809(6)	
Mo(5)-O(6)	1.821(7)	
Mo(5)-O(8)	1.997(7)	
Mo(5)-O(2)	2.020(6)	
Mo(5)-O(23)	2.617(7)	
Mo(5)-Mo(9)	**3.1978(15) => Mo^{VI}**	
Mo(6)-O(21)	1.672(7)	**Σ(Mo6) = 5.3**
Mo(6)-O(7)	1.948(6)	
Mo(6)-O(10)	1.966(7)	
Mo(6)-O(1)#1	2.019(6)	
Mo(6)-O(20)	2.024(7)	
Mo(6)-O(4)	2.504(6) => **Mo^{V}**	
Mo(7)-O(29)	1.681(7)	**Σ(Mo7) = 5.3**
Mo(7)-O(17)	1.942(8)	
Mo(7)-O(27)	1.955(7)	
Mo(7)-O(12)	1.971(7)	
Mo(7)-O(24)	2.050(7)	
Mo(7)-O(5)	2.530(7)	
Mo(7)-Mo(11)	**2.6310(16) => Mo^{V}**	
Mo(8)-O(37)	1.685(7)	**Σ(Mo8) = 6.1**
Mo(8)-O(20)	1.811(7)	
Mo(8)-O(13)	1.827(7)	
Mo(8)-O(19)	1.978(8)	
Mo(8)-O(31)	1.985(7)	
Mo(8)-O(4)	2.597(7)	
Mo(8)-Mo(12)	**3.1832(18) => Mo^{VI}**	
Mo(9)-O(32)	1.686(7)	**Σ(Mo9) = 6.0**
Mo(9)-O(24)	1.817(7)	
Mo(9)-O(33)	1.821(7)	
Mo(9)-O(2)	2.005(7)	
Mo(9)-O(8)	2.019(7)	
Mo(9)-O(5)	2.559(7) => **Mo^{VI}**	
Mo(10)-O(22)	1.672(7)	**Σ(Mo10) = 5.4**
Mo(10)-O(25)	1.952(7)	
Mo(10)-O(16)	1.953(8)	
Mo(10)-O(9)	1.975(7)	
Mo(10)-O(38)	2.035(8)	
Mo(10)-O(28)	2.497(7) => **Mo^{V}**	
Mo(11)-O(34)	1.682(7)	**Σ(Mo11) = 5.4**
Mo(11)-O(25)	1.955(7)	
Mo(11)-O(12)	1.958(7)	
Mo(11)-O(17)	1.962(7)	
Mo(11)-O(39)	2.011(8)	
Mo(11)-O(28)	2.554(7) => **Mo^{V}**	
Mo(12)-O(40)	1.677(8)	**Σ(Mo12) = 6.1**
Mo(12)-O(39)	1.813(8)	
Mo(12)-O(38)	1.816(7)	
Mo(12)-O(31)	2.016(7)	
Mo(12)-O(19)	2.025(7)	
Mo(12)-O(28)	2.554(7) => **Mo^{V}**	

Figure SI5. Two views showing the connecting mode of an εZn POM to the four neighboring POMs in **ε(isop)$_2$** and **Z-POMOF1**; the blue {PZn_4} tetrahedra schematize the POMs.

ε(isop)$_2$

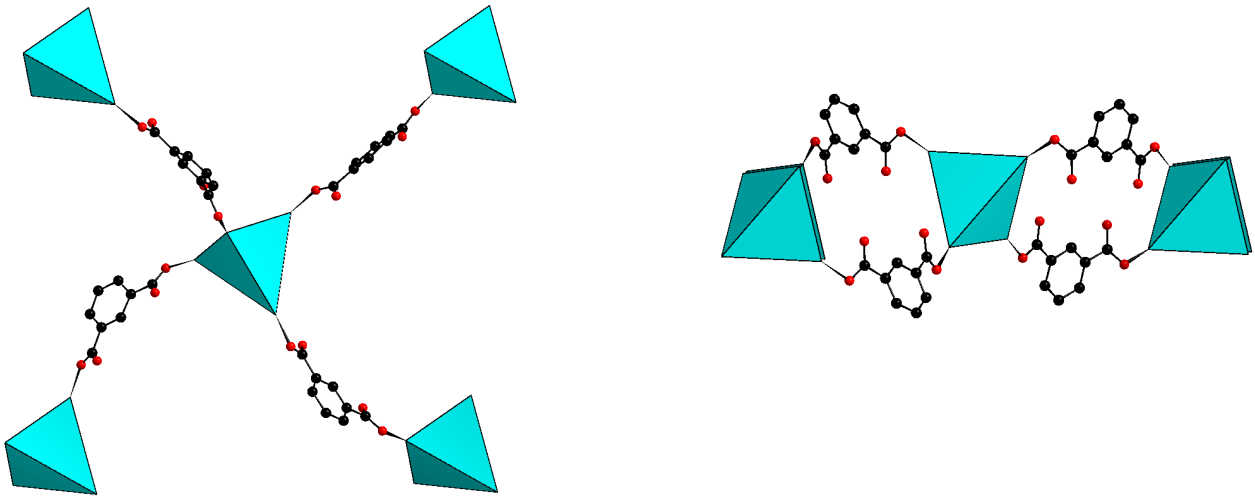

Z-POMOF1

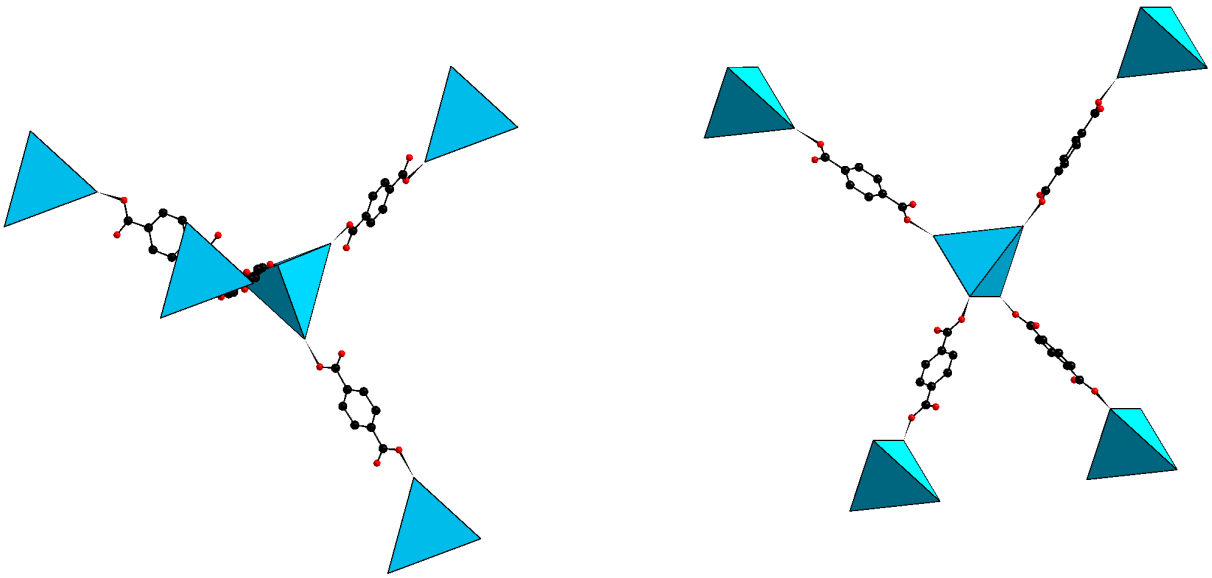

Figure SI6. Views along the *c* and *b* axis of the unit-cell of **ε(isop)$_2$** showing the stacking of the 2D planes.

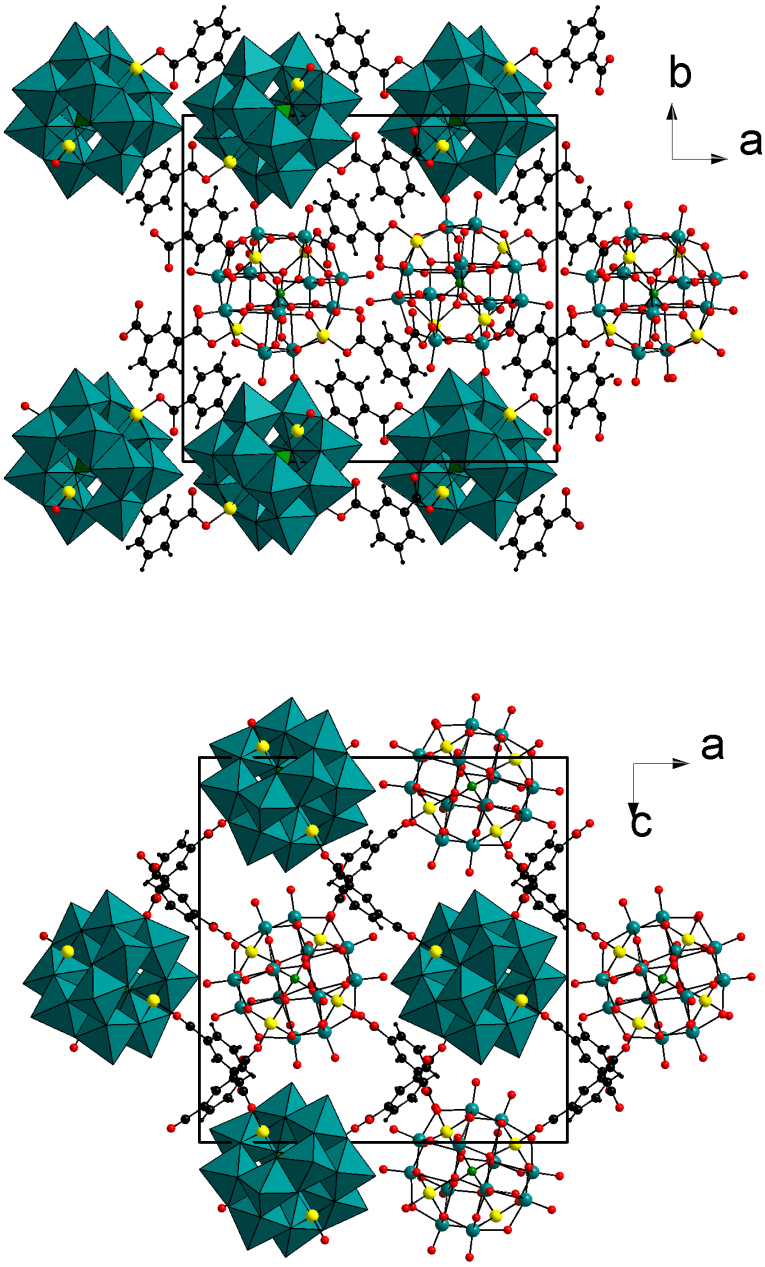

Figure SI7. View along the *a* axis of the unit-cell of **ε(bim)$_4$**.

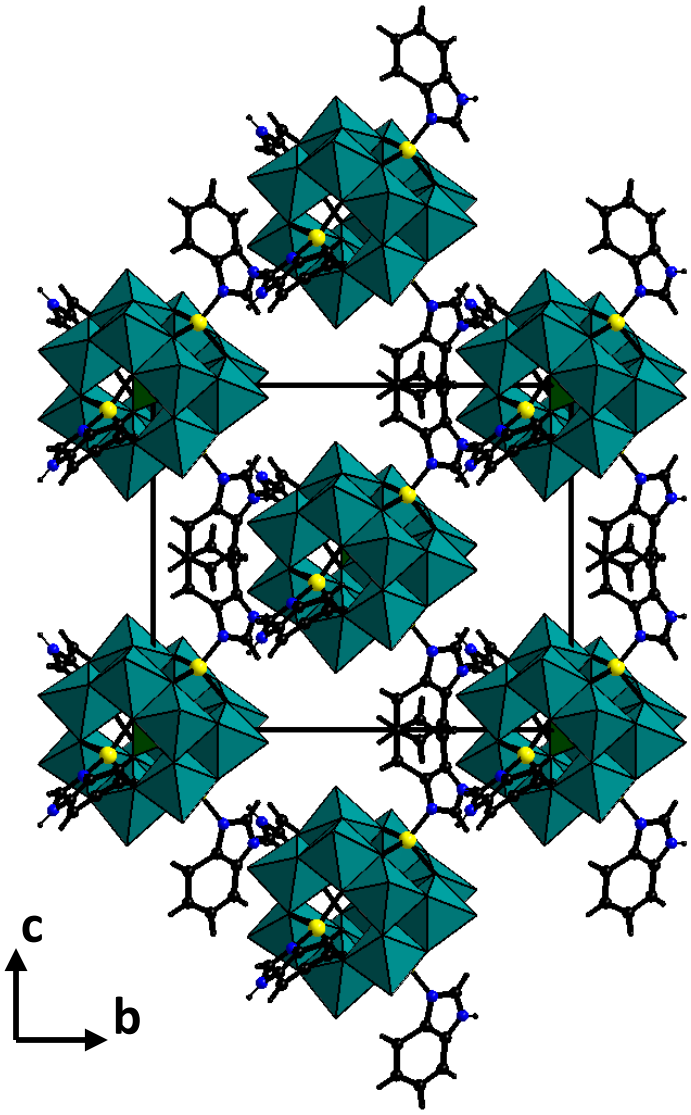

Figure SI8. Hypothetical structure built from the connection of the εZn units of **ε(bim)$_4$** in which half of the ligands have been removed.

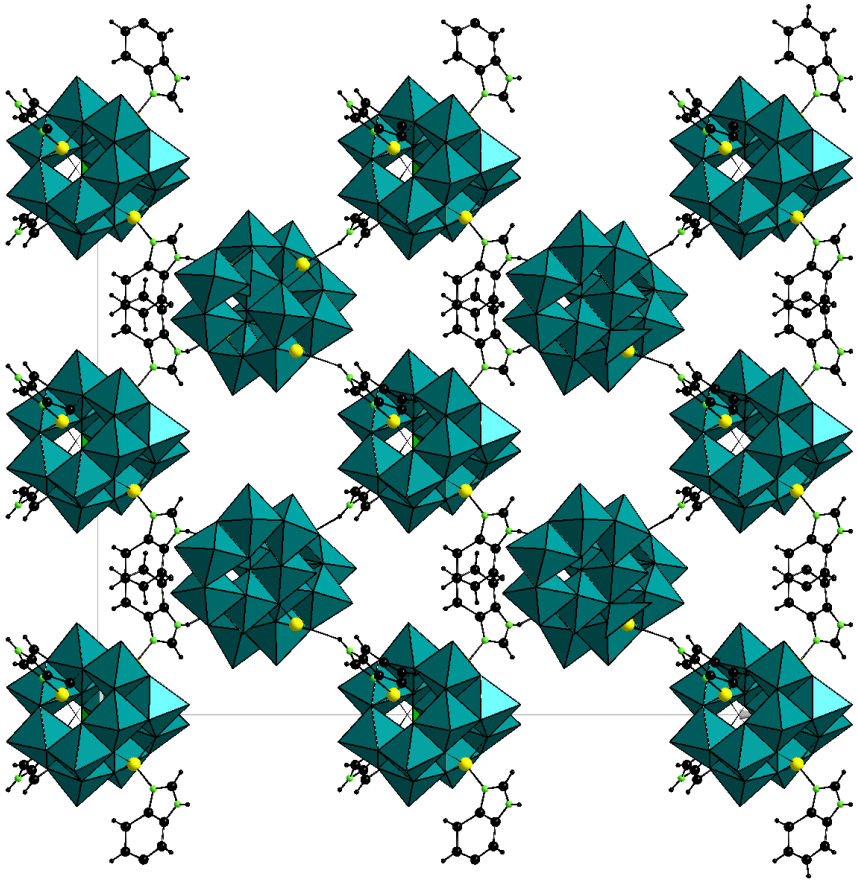

Figure SI9. View of the dimeric inorganic building unit in **ε_2(pazo)$_4$**.

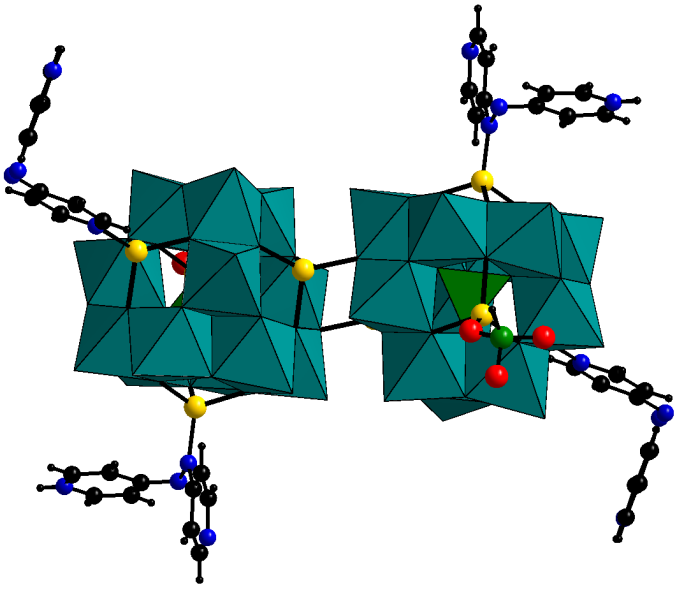

Figure SI10. Trimers of pazo ligands in π-π interactions in **ε_2(pazo)$_4$**.

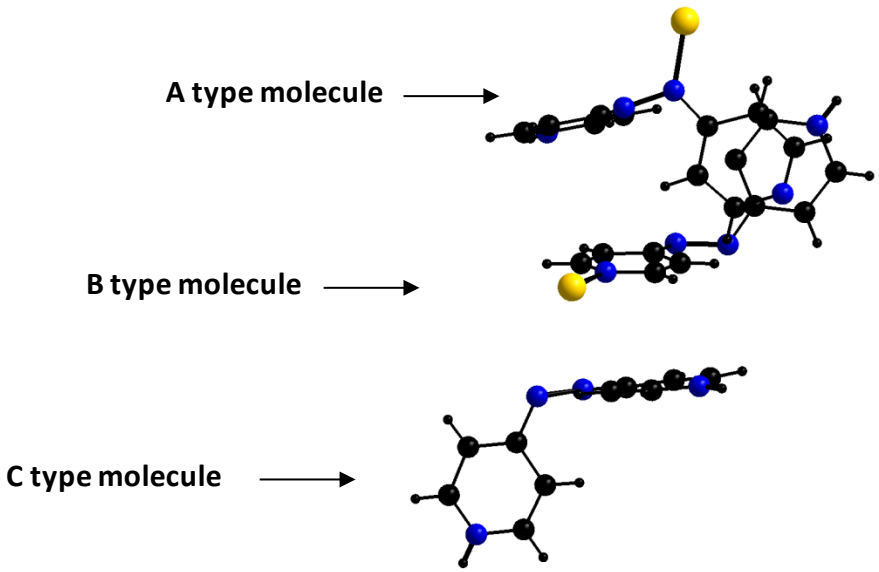

Figure SI11. Comparison of the experimental X-ray powder patterns (in black) and of the powder pattern calculated from the structure solved from single-crystal X-ray diffraction data (in red).

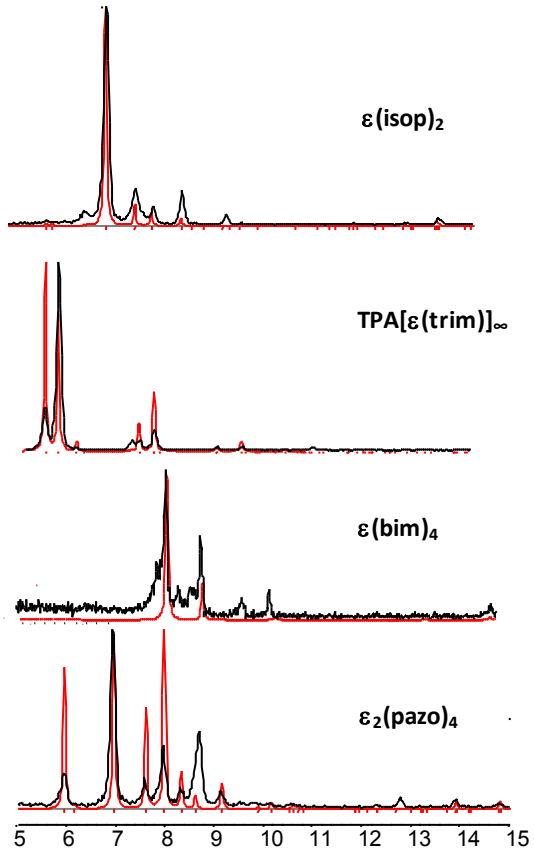

Figure SI12: XPS spectra of Mo3d of as-prepared **ε₂(pazo)₄**@G.

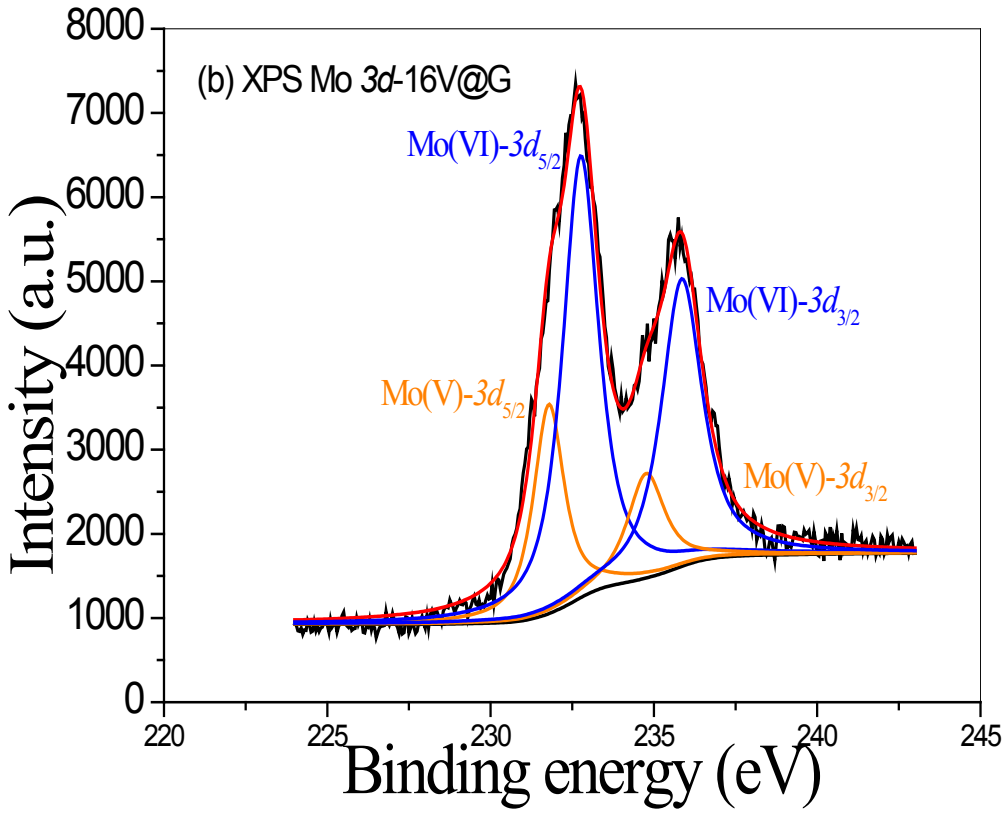

Figure SI13: Raman spectra of natural G, GO before reaction and as-prepared **ε$_2$(pazo)$_4$**@G.

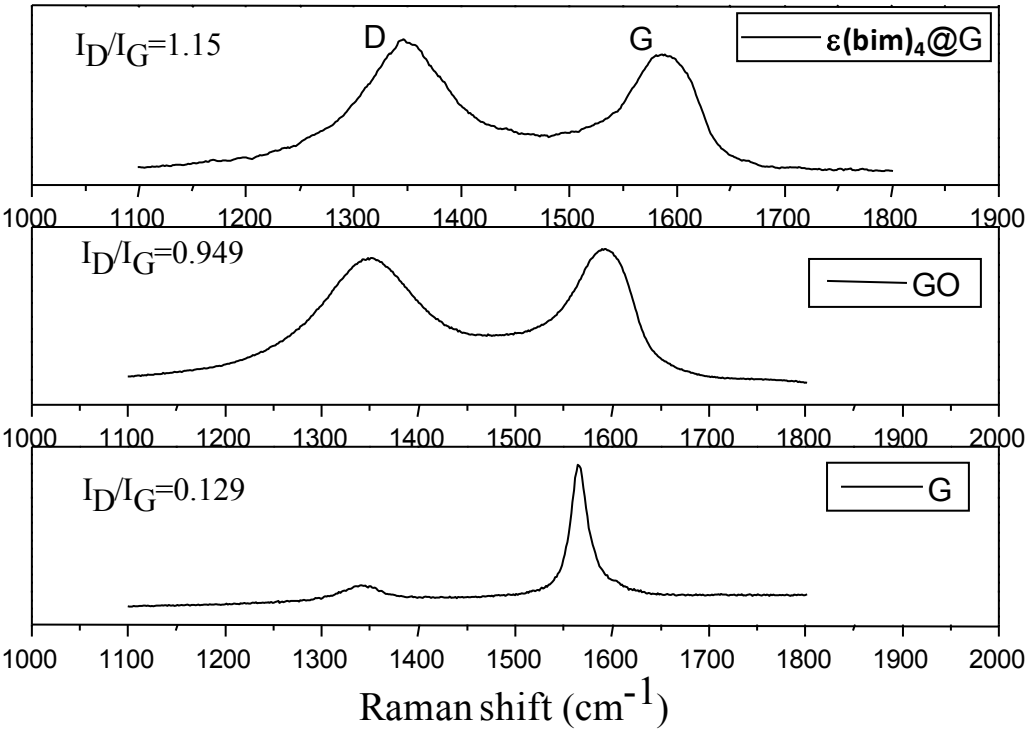

Figure SI14: Experimental X-Ray powder pattern of the GO precursor used in this study.

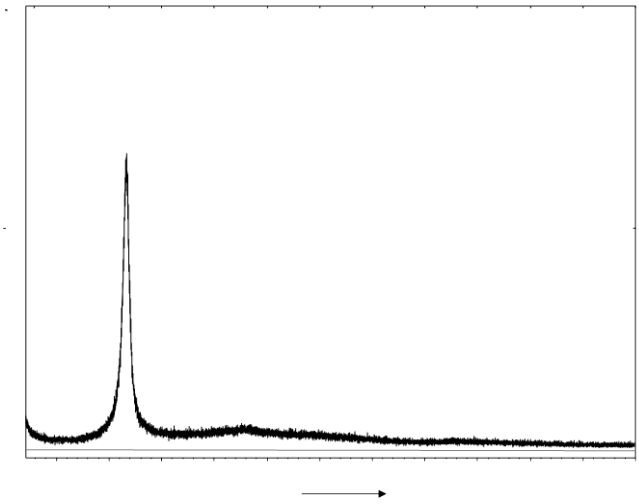

Figure SI15: Top: comparison of the experimental X-ray powder pattern (in black) of **ε_2(pazo)$_4$**@G and of the powder pattern calculated from the structure solved from single crystal X-ray diffraction data for **ε_2(pazo)$_4$** (in red). Bottom : comparison of the experimental X-ray powder pattern (in black) of **ε(isop)$_2$**@G and of the powder pattern calculated from the structure solved from single crystal X-ray diffraction data (in red) for **ε(isop)$_2$**.

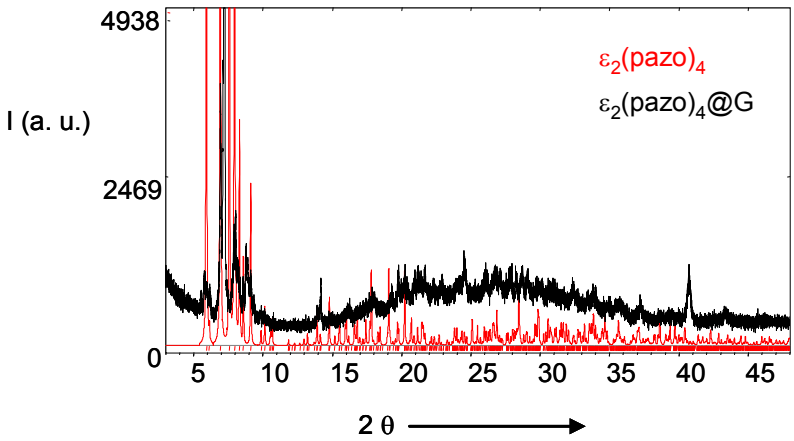

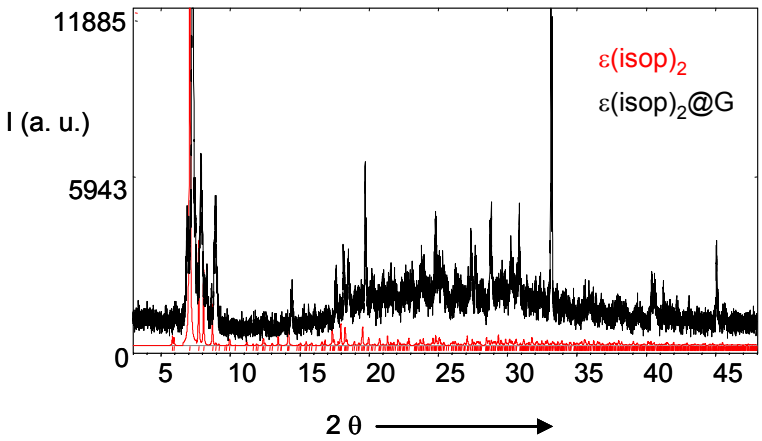

Figure SI16: Infrared spectra of the POMOF **ε(isop)$_2$** (in purple) and of the **ε(isop)$_2$**@G material (in red).

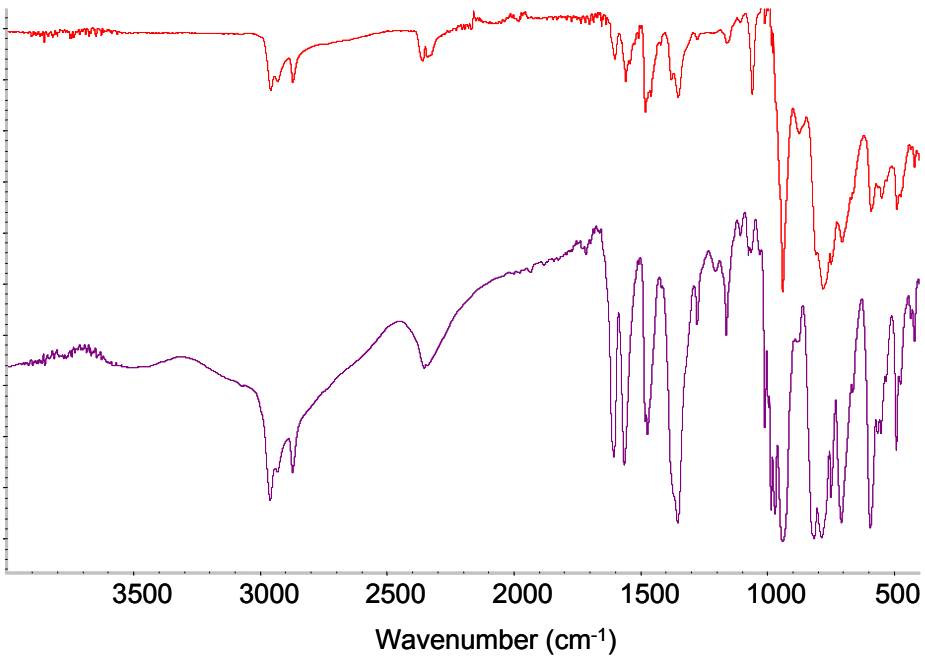

Figure SI17: Infrared spectra of the POMOF **ε$_2$(pazo)$_4$** (in purple) and of the **ε$_2$(pazo)$_4$**@G material (in red).

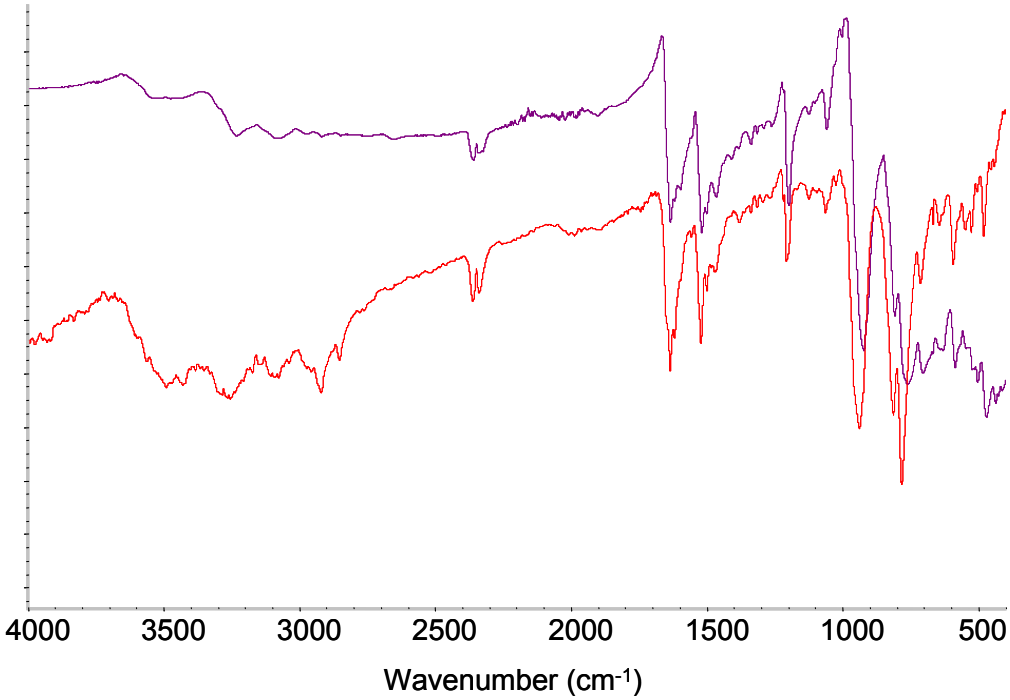

Figure SI18: TEM images of GO (a) and as-prepared **ε(isop)$_2$@G** nanohybrid (b); SEM image of **ε(isop)$_2$@G** nanohybrid (c); EDX analysis of **ε(isop)$_2$@G** nanohybrid (d).

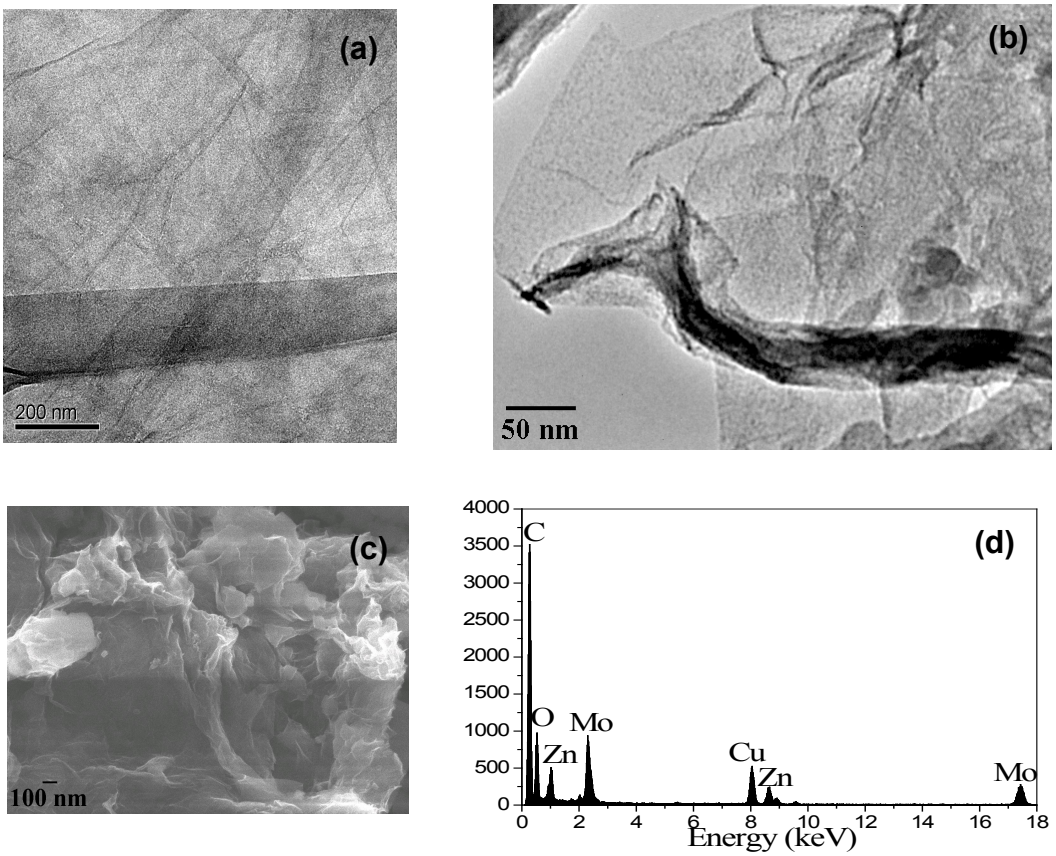

Figure SI19: SEM image (a) and TEM (b) image of as-prepared **ε_2(pazo)4@G** nanohybrid.

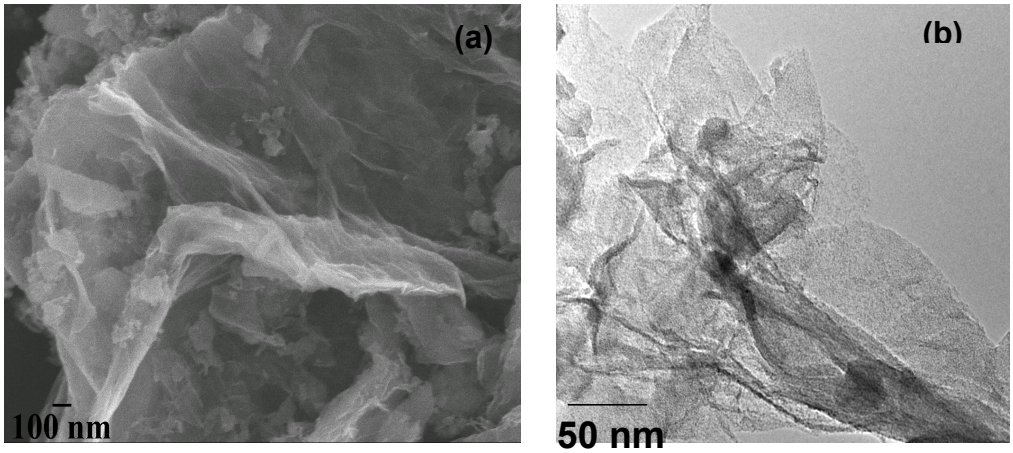

Figure SI20: Superposition of the 1st and 5000th cyclic voltammograms recorded with **ε(isop)$_2$@G** in a (1M LiCl +HCl (pH 1)) medium.The scan rate was100 mV s^{-1}. The reference electrode was a saturated calomel electrode (SCE).